

This is the accepted manuscript made available via CHORUS. The article has been published as:

High-temperature multiferroicity and strong magnetocrystalline anisotropy in 3d-5d double perovskites

Marjana Ležaić and Nicola A. Spaldin

Phys. Rev. B **83**, 024410 — Published 25 January 2011

DOI: [10.1103/PhysRevB.83.024410](https://doi.org/10.1103/PhysRevB.83.024410)

High temperature multiferroicity and strong magnetocrystalline anisotropy in $3d - 5d$ double perovskites

Marjana Ležaić^{1,2} and Nicola A. Spaldin²

¹*Institut für Festkörperforschung, Forschungszentrum Jülich, D-52425 Jülich and JARA-FIT, Germany**

²*Department of Materials, ETH Zurich, Wolfgang-Pauli Strasse 10, CH-8093 Zurich, Switzerland*

Using density functional calculations we explore the properties of as-yet-unsynthesized $3d - 5d$ ordered double perovskites ($A_2BB'O_6$) with highly polarizable Bi^{3+} ions on the A site. We find that the Bi_2NiReO_6 and Bi_2MnReO_6 compounds are insulating and exhibit a robust net magnetization that persists above room temperature. When the in-plane lattice vectors of the pseudocubic unit cell are constrained to be orthogonal (for example by coherent heteroepitaxy), the ground states are ferroelectric with large polarization and a very large uniaxial magnetocrystalline anisotropy with easy axis along the ferroelectric polarization direction. Our results suggest a route to multiferroism and electrically controlled magnetization orientation at room temperature.

PACS numbers: 75.85.+t, 77.55.Nv

I. INTRODUCTION

There is increasing current interest in developing multiferroic materials with ferromagnetic and ferroelectric order in the same phase for future spintronic or magneto-electronic devices¹⁻⁴. Although new multiferroics are being predicted and synthesized at an accelerating pace, a major obstacle for their adoption in applications remains their low magnetic ordering temperatures, which are generally far below room temperature. The problem more generally lies in the scarcity of insulators with any net magnetization – either ferro- or ferrimagnetic – at room temperature, even before the additional requirement of polarization is included. Most work on novel multiferroics has been restricted to $3d$ transition metal oxides (see for example⁵⁻¹²), motivated by the expectation that $4d$ or $5d$ compounds would likely be metallic. However, recent work on new $3d - 5d$ double perovskites^{13,14} showed this to be a misconception, and identified a ferrimagnetic insulator, Sr_2CrOsO_6 , with magnetic ordering temperature well above room temperature. First-principles calculations have been shown to accurately reproduce the measured magnetic ordering temperatures^{15,16}, in the Sr_2CrMO_6 series ($M = W, Re, Os$)¹⁷, and have been invaluable in explaining the origin of the robust ferrimagnetic ordering¹⁸⁻²¹.

We build here on these recent developments to propose a route to achieving multiferroics with higher magnetic ordering temperatures. We use $3d - 5d$ double perovskites to achieve high temperature magnetism combined with insulating behavior, and introduce lone-pair active cations on the A sites to induce polarizability^{22,23}. The heavy Bi and $5d$ elements provide an additional desirable feature: The spin-orbit interaction strongly couples the magnetic easy axis to the ferroelectric polarization direction. Specifically, we explore two compounds, Bi_2MnReO_6 and Bi_2NiReO_6 . We use density functional theory to calculate their zero Kelvin structure and magnetic ordering, and Monte Carlo simulations with parameters extracted from the first-principles calculations to

calculate their magnetic ordering temperatures. We find that both materials are magnetic insulators, with ordering temperatures well above room temperature. While the global ground state in both materials is anti-polar, we show that when the in-plane lattice vectors form an angle close to 90° a ferroelectric phase results. In practice this could be achieved using coherent heteroepitaxy and the resulting ferroelectricity could be manipulated using strain. We show that the magnetic behavior results from an antiferromagnetic superexchange^{17,24} and the ferroelectricity from the Bi^{3+} lone pairs, reminiscent of other Bi-based multiferroics. Finally, we investigate the effect of strong spin-orbit coupling (SOC) due to the presence of heavy Bi^{3+} and Re^{4+} cations on the structural, magnetic and ferroelectric properties of these compounds.

II. METHOD OF CALCULATION

Structural optimizations were performed using the Vienna *Ab-initio* Simulation Package (VASP) with PAW PBE potentials²⁵; the semicore p states of Mn, Ni and Re and the d states of Bi were included in the valence. We used an energy cutoff of 500 eV and $6 \times 6 \times 6$, $4 \times 4 \times 6$ and $4 \times 4 \times 4$ Γ -point centered k-point meshes for unit cells containing 10, 20 and 40 atoms respectively. The exchange-correlation functional was treated within the generalized gradient approximation (GGA)²⁶; while extension to the GGA+ U method had only a small influence on the electronic properties, we discuss later its effect on the structural behavior. Magnetic ordering temperatures were obtained using a finite-temperature Monte Carlo scheme within a Heisenberg Hamiltonian $H = -\frac{1}{2} \sum_{i,j} J_{i,j} \mathbf{M}_i \cdot \mathbf{M}_j$, where $\mathbf{M}_i, \mathbf{M}_j$ are the magnetic moments on sites i and j of the crystal lattice. The exchange constants $J_{i,j}$ were calculated in the frozen-magnon scheme²⁷ using the all-electron full-potential linearized augmented plane-wave code, FLEUR²⁸, with a plane-wave cut-off of 4.2 hartrees and $15 \times 15 \times 15$ k-points and a $6 \times 6 \times 6$ spin-spiral grid in a 10-atom unit

cell. Ferroelectric polarizations were extracted from the shifts of the centers of Wannier functions²⁹. The magnetocrystalline anisotropy energy was extracted from the self-consistent total-energy calculations within the FLEUR code, on a $13 \times 13 \times 13$ k-points grid.

First, we calculate the lowest energy structure for both $\text{Bi}_2\text{MnReO}_6$ and $\text{Bi}_2\text{NiReO}_6$ within the GGA approximation. We proceed by successively freezing in the 12 centrosymmetric combinations of tilts and rotations of the oxygen octahedra that can occur in ordered double perovskites³⁰. We then further reduce the symmetry of these lowest energy tilt systems by displacing the anions and cations relative to each other in the manner of a polar displacement. Next we optimize the atomic positions (by minimizing the Hellmann-Feynman forces), as well as the unit cell shape and volume within each symmetry. In this first series of optimizations we assume ferrimagnetic ordering and do not include SOC; the influence of the SOC on the lowest-energy structures is examined later.

III. GROUND-STATE STRUCTURE AND INFLUENCE OF EPITAXIAL CONSTRAINTS

Our calculations yield the same monoclinic, centrosymmetric $P2_1/n$ symmetry ground state for both compounds. It is characterized by an $a^-a^-c^+$ tilt pattern of the oxygen octahedra. Two lattice vectors are identical with angles of 93.6° and 93.5° between them in the Mn and Ni compounds respectively (in the following we refer to these as the “in-plane” lattice vectors); the third lattice vector is perpendicular to the first two and of different length. Importantly, in both compounds there is a slightly higher energy ferroelectric (FE) structure with rhombohedral $R3$ symmetry (see Tab. I). The $R3$ structure corresponds to an $a^-a^-a^-$ tilt pattern yielding lattice vectors of equal length and rhombohedral angles of 60° and 61° for the Mn and Ni compounds respectively, combined with polar relative displacements of anions and cations along the $[111]$ rhombohedral axis induced by the well-established stereochemically active Bi lone pair²² (see Fig. 1). The energy of the FE phase is significantly lower than that of the corresponding centrosymmetric $R\bar{3}$ phase, suggesting a high ferroelectric ordering temperature if this symmetry could be stabilized. For comparison, in the prototypical multiferroic BiFeO_3 with T_C of 1103 K, we obtain a difference of

Symmetry	Tilt system (in Glazer notation ³¹)	Total energy	
		$\text{Bi}_2\text{MnReO}_6$	$\text{Bi}_2\text{NiReO}_6$
$Fm\bar{3}m$	$a^0a^0a^0$	1.86 eV	2.02 eV
$R\bar{3}$	$a^-a^-a^-$	248 meV	333 meV
$R3$	$a^-a^-a^- + \text{FE shift}$	32 meV	18 meV

TABLE I: Total energies (per formula unit) of the lowest-energy phases of $\text{Bi}_2\text{MnReO}_6$ and $\text{Bi}_2\text{NiReO}_6$ and the cubic $Fm\bar{3}m$ phase with respect to their ground state $P2_1/n$ phase.

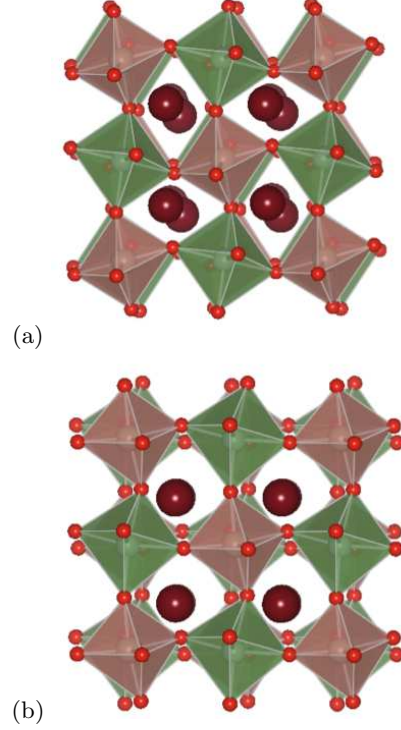


FIG. 1: (color online) (a) Ground-state $P2_1/n$ structure and (b) the ferroelectric $R3$ structure of the double perovskites $\text{Bi}_2\text{MnReO}_6$ and $\text{Bi}_2\text{NiReO}_6$. Bi^{3+} cations are depicted as the large brown spheres and O^{2-} as the small red spheres. Re^{4+} and Mn^{2+} (Ni^{2+}) are alternating in the shaded octahedra, in a 3-dimensional checkerboard manner (this is indicated by the color of the octahedra). While in the $P2_1/n$ symmetry the Bi^{3+} cations form an “anti-polar” pattern, their coherent shift along the $[111]$ direction can be clearly seen in the $R3$ structure.

515 meV per two formula units between the corresponding states. The calculated polarization in both cases is along the $[111]$ direction, and comparable in size to that of BiFeO_3 (see Tab. II).

While the ground state $P2_1/n$ phase is of interest in its own right as a possible high temperature magnetic insulator, we next explore whether it is possible to identify conditions that stabilize the $R3$ ferroelectric phase. We use the fact that in the FE $R3$ phase all three lattice vectors have equal length, and the rhombohedral angle is equal or close to the ideal value of 60° . In contrast, in the $P2_1/n$ phase, only the lengths of the two in-plane lattice vectors are equal, and the inter-in-plane angles deviate strongly from the ideal 90° . Motivated by these observations, we first constrain all three lattice parameters to be equal in length and indeed find that this constraint stabilizes the FE phase. Next we enforce that only two of the three lattice parameters are equal in length, but constrain them to be perpendicular to each other and again find that the FE phase is the lowest energy³⁷. Such a constraint could be achieved in practice through coher-

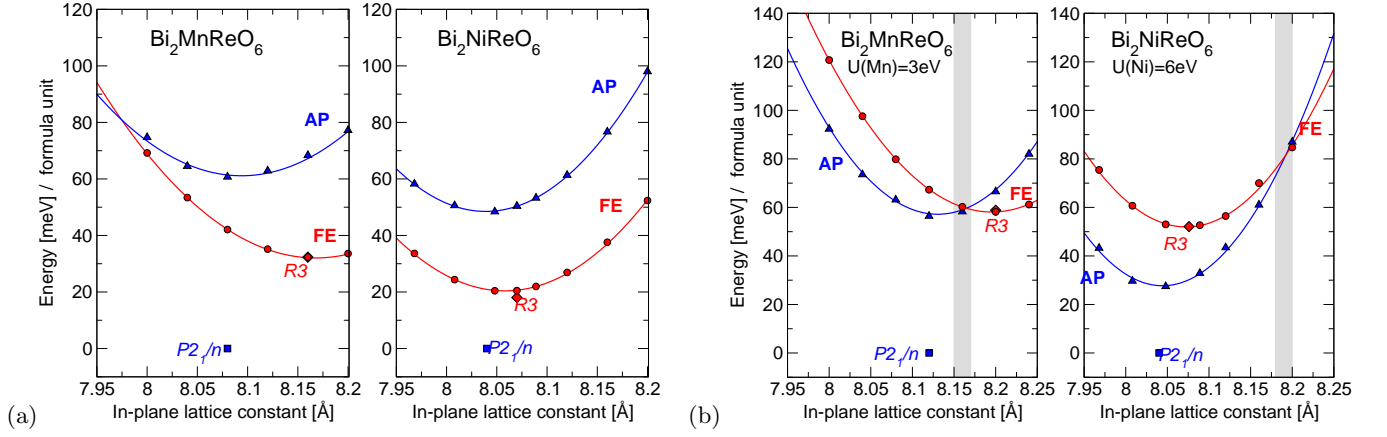


FIG. 2: (color online) (a) Distorted $\text{Bi}_2\text{MnReO}_6$ and $\text{Bi}_2\text{NiReO}_6$ obtained from the $R3$ (red circles) and $P2_1/n$ (blue triangles) structure by constraining the two in-plane lattice vectors to be equal, and the angle between them to 90° . The out-of-plane parameter and the ionic positions were relaxed. The energies are positioned with respect to the bulk unconstrained $P2_1/n$ ground state (blue squares). The red diamonds show the energies for the unconstrained $R3$ structure. A crossover between the anti-polar (AP) and the ferroelectric (FE) state occurs at 1.8% (with respect to the minimum of the FE curve) of compressive strain in $\text{Bi}_2\text{MnReO}_6$. Note that the energy of the $R3$ state lies on the strain curve for $\text{Bi}_2\text{MnReO}_6$, but is somewhat lower for $\text{Bi}_2\text{NiReO}_6$, due to the choice of a square in-plane lattice: the rhombohedral angle in $R3$ phase of $\text{Bi}_2\text{MnReO}_6$ is 60° , while in $\text{Bi}_2\text{NiReO}_6$ it is 61° . (b) Similar to (a), with an addition of a Hubbard U on Mn (3 eV) and Ni (6 eV) 3d states. The shaded area shows the AP-FE crossover region.

ent heteroepitaxy between a thin film and a substrate, and is often described as a biaxial strain state in the literature. In Fig. 2(a), we show the calculated energies of the previously $R3$ and $P2_1/n$ structure types subject to this additional constraint, with the in-plane lattice parameters varied over a range of realistic substrate strains corresponding to (001) epitaxial growth. For each in-plane lattice parameter we allow the length and angle of the out-of-plane lattice parameter and atomic positions to relax to their lowest-energy configurations. Our main finding is that, under the investigated constraint, the ferroelectric (FE) phase is lower in energy than the anti-polar (AP) phase. At the optimized value of in-plane lattice parameter (8.16 Å for $\text{Bi}_2\text{MnReO}_6$ and 8.07 Å for $\text{Bi}_2\text{NiReO}_6$) the energy differences between the FE and AP phases are 36 meV and 30 meV per formula unit respectively. The FE phases are robustly insulating with calculated band gaps of 0.7 eV and 0.3 eV respectively, and have large polarizations of $84 \mu\text{C}/\text{cm}^2$ ($\text{Bi}_2\text{MnReO}_6$) and $81 \mu\text{C}/\text{cm}^2$ ($\text{Bi}_2\text{NiReO}_6$) along the pseudocubic [111] direction. Notice, however, that as in-plane compressive strain is applied, the differences in energies reduce, and in fact in $\text{Bi}_2\text{MnReO}_6$ a cross-over is reached at compressive strain value of 1.8%. We therefore expect that both compounds, although anti-polar in bulk, will in fact be ferroelectric and hence multiferroic in thin-film form, over a range of experimentally accessible strains. We will see later that SOC tips the scale towards the FE phase, while electron correlations favor the AP phase.

IV. ELECTRONIC AND MAGNETIC PROPERTIES OF THE FERROELECTRIC PHASE

Next, we analyze the magnetic behavior of the two ferroelectric compounds. We find that in both cases the lowest energy ordering is ferrimagnetic, with the moments on the 3d and 5d transition metal ions anti-aligned (see Fig. 3). In both compounds, Re is in formal oxidation state 4^+ corresponding to a filled $d - t_{2g}$ manifold in the minority spin-channel. The oxidation states of Mn in $\text{Bi}_2\text{MnReO}_6$ and of Ni in $\text{Bi}_2\text{NiReO}_6$ are 2^+ ; $t_{2g}^3 e_g^2$ (high spin) for Mn and $t_{2g}^6 e_g^2$ for Ni. Due to these specific configurations of the outer electronic shells, and the nearly 150° Mn-O-Re (Ni-O-Re) angle, the magnetic moments on Re and Mn/Ni are coupled via an antiferromagnetic superexchange mechanism^{33–35}. The result is a ferrimagnetic configuration with a total spin moment of $2 \mu_B$ in $\text{Bi}_2\text{MnReO}_6$ and $1 \mu_B$ in $\text{Bi}_2\text{NiReO}_6$.

Our calculated magnetic ordering temperatures in the ferroelectric phase are 330 K for $\text{Bi}_2\text{MnReO}_6$ and 360 K for $\text{Bi}_2\text{NiReO}_6$, both significantly above room temperature. As a comparison, using the same method, we calculate a magnetic ordering temperature of 670 K for $\text{Sr}_2\text{CrOsO}_6$ (the experimental value is 725 K). Note that if growth can only be achieved in the form of ultra-thin films, the ordering temperatures will likely be reduced.

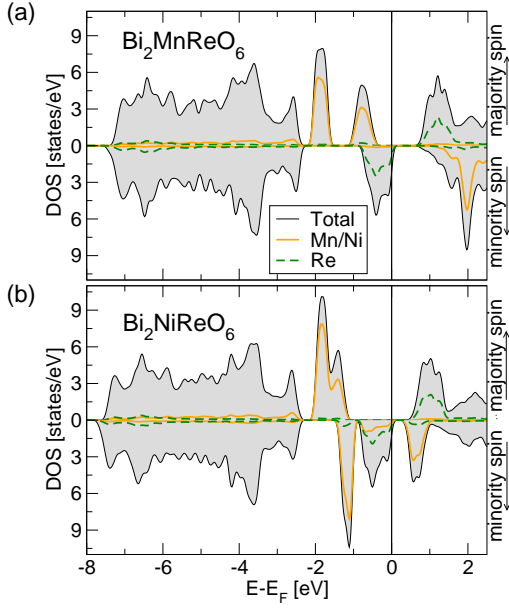


FIG. 3: (color online) Density of states (DOS) of the ferroelectric phase of $\text{Bi}_2\text{MnReO}_6$ (a) and $\text{Bi}_2\text{NiReO}_6$ (b). The local magnetic moments on Mn/Ni and Re are anti-aligned. Thin black line: total DOS, green dashed line: Re, orange solid line: Mn/Ni.

V. SPIN-ORBIT COUPLING AND CORRELATIONS EFFECTS

Since the heavy Re and Bi atoms in our double perovskites are also likely to exhibit strong SOC, and consequently significant magneto-structural coupling¹⁸, we repeat our calculations with SOC explicitly included. We find that the ground state remains $P2_1/n$ AP, but now its energy difference from the FE state with $R3$ symmetry is reduced to 10 meV in $\text{Bi}_2\text{MnReO}_6$ and only 2 meV in $\text{Bi}_2\text{NiReO}_6$. Both compounds still have semiconducting gaps which are now somewhat reduced while the ferroelectric polarization of the $R3$ phase is slightly increased (see Tab.II). The total magnetic moments (spin+orbital) amount to $2.34 \mu_B$ and $0.58 \mu_B$ respectively. Note that, in contrast to half-metallic ferromagnets where the SOC introduces states in the minority-spin gap yielding a non-integer total magnetic moment, here the non-integer moment is the consequence of the mixing of spin-up and spin-down states (spin is no longer a good quantum number with SOC included), while the gap is preserved.

In both compounds the magnetic easy axis lies along the ferroelectric polarization direction. The associated anisotropy energy is large and comparable to that in current magnetic recording media: it amounts to 7 meV and 5.5 meV per formula unit in $\text{Bi}_2\text{MnReO}_6$ and $\text{Bi}_2\text{NiReO}_6$, respectively. This suggests an exciting possibility of electrical control of the magnetization direction.

Finally, we investigate the influence of electronic correlations by adding a Hubbard U on the d states of Mn

SOC	Compound	band gap [eV]	P [$\mu\text{C}/\text{cm}^2$]	M [$\mu_B/\text{f.u.}$]
off	$\text{Bi}_2\text{MnReO}_6$	0.7	84	2
	$\text{Bi}_2\text{NiReO}_6$	0.3	78	1
on	$\text{Bi}_2\text{MnReO}_6$	0.4	86	2.34
	$\text{Bi}_2\text{NiReO}_6$	0.2	80	0.58

TABLE II: Properties of the bulk ferroelectric $R3$ phase in $\text{Bi}_2\text{MnReO}_6$ and $\text{Bi}_2\text{NiReO}_6$ with and without the SOC included: band gap, ferroelectric polarization P and the total magnetic moment M (spin+orbital in case of SOC) per formula unit (f.u.).

and Ni. In order to reduce the computational effort, we do not include the SOC. We keep in mind, however, that a consequence of its inclusion, as we have seen, is a reduction in the energy of the FE state with respect to the AP one. Introduction of Hubbard U corrections (on Mn $U=3$ eV and $J=0.87$ eV, and on Ni $U=6$ eV and $J=0.90$ eV) does not change the ground state structure ($P2_1/n$ still has the lowest energy). Interesting quantitative changes occur in the strain dependence however (Fig. 2(b)). While within the GGA the ferroelectricity was robust to the choice of substrate lattice parameters over a likely range of accessible strains provided that the in-plane lattice parameters were constrained to be perpendicular to each other, in GGA+ U we find a cross-over between the FE and AP states at moderate strain values. This suggests the intriguing possibility that an external strain, for example from a piezoelectric substrate³⁶ could induce a “dipole-flop” transition from a non-polar structure in which the dipoles are anti-aligned to a ferroelectric one. For the assumed value of U , the crossover region (shaded area in Fig 2(b)) in $\text{Bi}_2\text{MnReO}_6$ is within less than 1% from either of the two minima: a small compressive strain will push the system towards the AP state, while a small tensile strain will favor a FE state. In $\text{Bi}_2\text{NiReO}_6$ the applied U pushes the AP state lower in energy, but the crossover region to the FE state is still within an experimentally accessible range of 1.5% tensile strain. While we can not make a quantitative prediction, since the relative energies of the AP and the FE state depend strongly on the value of the applied U correction, within a reasonable range of U the crossover region lies within 2% strain from the ground state structure.

VI. CONCLUSION

In summary, we predict from first-principles calculations that the $3d-5d$ double-perovskite compounds $\text{Bi}_2\text{MnReO}_6$ and $\text{Bi}_2\text{NiReO}_6$ are high- T_C ferrimagnetic insulators. Moreover, it is likely possible to stabilize them in thin-film form in a ferroelectric phase with high polarization along the $[111]$ direction. The magnetic easy axis lies along the ferroelectric polarization direction with a very large associated anisotropy energy. The different sizes and charges of the $3d$ and $5d$ transition metal ions

suggest that the required B-site ordering should be experimentally feasible; we hope that our findings will initiate experimental efforts to synthesize these novel multiferroic compounds.

We thank Drs. Kris Delaney, Phivos Mavropoulos, Stefan Blügel, Frank Freimuth and Sergey Ivanov for many valuable discussions. M.L. gratefully acknowledges the support of Deutsche Forschungsgemeinschaft, grant LE 2504/1-1, and the Young Investigators Group Programme of Helmholtz Association, contract VH-NG-409, as well as the Jülich Supercomputing Centre. NS acknowledges support from the NSF NIRT program, grant number 0609377.

* Electronic address: m.lezaic@fz-juelich.de

- ¹ Xi Chen, A. Hochstrat, P. Borisov, and W. Kleemann, *Appl. Phys. Lett.* **89**, 202508 (2006).
- ² M. Gajek, M. Bibes, S. Fusil, K. Bouzehouane, J. Fontcuberta, A. Barthélémy, and A. Fert, *Nature Mat.* **6**, 296 (2007).
- ³ Ying-Hao Chu, Lane W. Martin, Mikel B. Holcomb, Martin Gajek, Shu-Jen Han, Qing He, Nina Balke, Chan-Ho Yang, Donkoun Lee, Wei Hu, Qian Zhan, Pei-Ling Yang, Arantxa Fraile-rodriguez, Andreas Scholl, Shan X. Wang and R. Ramesh, *Nature Mat.* **7**, 478 (2008).
- ⁴ D. Lebeugle, A. Mougin, M. Viret, D. Colson, and L. Ranno, *Phys. Rev. Lett.* **103**, 257601 (2009)
- ⁵ Kunihiko Yamauchi, Tetsuya Fukushima, and Silvia Picozzi, *Phys. Rev.* **79**, 212404 (2009).
- ⁶ S. Picozzi, K. Yamauchi, B. Sanyal, I. A. Sergienko, and E. Dagotto, *Phys. Rev. Lett.* **99**, 227201 (2007)
- ⁷ Gianluca Giovannetti, Sanjeev Kumar, Jeroen van den Brink, and Silvia Picozzi, *Phys. Rev. Lett.* **103**, 037601 (2009)
- ⁸ Y. Yamasaki, S. Miyasaka, Y. Kaneko, J.-P. He, T. Arima and Y. Tokura, *Phys. Rev. Lett.* **96**, 207204 (2006)
- ⁹ P. Baettig, C. Ederer, and N. A. Spaldin, *Phys. Rev. B* **72**, 214105 (2005).
- ¹⁰ R. Nechache, C. Harnagea, L.-P. Carignan, O. Gautreau, L. Pintilie, M. P. Singh, D. Menard, P. Fournier, M. Alexe, and A. Pignolet, *et al.*, *J. Appl. Phys.* **105**, 061621 (2009).
- ¹¹ A. J. Hatt, N. A. Spaldin and C. Ederer, *Phys. Rev. B* **81**, 054109 (2010).
- ¹² M. Sakai, A. Masuno, D. Kan, M. Hashisaka, K. Takata, M. Azuma, M. Takano, and Y. Shimakawa, *et al.*, *Appl. Phys. Lett.* **90**, 072903 (2007)
- ¹³ Y. Krockenberger, K. Mogare, M. Reehuis, M. Tovar, M. Jansen, G. Vaitheeswaran, V. Kanchana, F. Bultmark, A. Delin, F. Wilhelm, A. Rogalev, A. Winkler, and L. Alff, *Phys. Rev. B* **75**, 020404R (2007).
- ¹⁴ K.-W. Lee and W. E. Pickett, *Phys. Rev. B* **77**, 115101 (2008).
- ¹⁵ J. B. Philipp, P. Majewski, L. Alff, A. Erb, R. Gross, T. Graf, M. S. Brandt, J. Simon, T. Walther, W. Mader, D. Topwal, and D. D. Sarma, *Phys. Rev. B* **68**, 144431 (2003).
- ¹⁶ H. Kato, T. Okuda, Y. Okimoto, Y. Tomioka, Y. Takenoya, A. Ohkubo, M. Kawasaki, and Y. Tokura, *Appl. Phys. Lett.* **81**, 328 (2002).
- ¹⁷ Tapas Kumar Mandal, Claudia Felser, Martha Greenblatt, and Jürgen Kübler, *Phys. Rev. B* **78**, 134431 (2008).
- ¹⁸ D. Serrate, J. M. De Teresa and M. R. Ibarra, *J. Phys.:Condens.Matter* **19**, 023201 (2007).
- ¹⁹ D. D. Sarma, P. Mahadevan, T. Saha-Dasgupta, S. Ray, and A. Kumar, *Phys. Rev. Lett.* **85**, 2549 (2000).
- ²⁰ J. Kanamori and K. Terakura, *J. Phys. Soc. Jpn.* **70**, 1433 (2001).
- ²¹ Z. Fang, K. Terakura, and J. Kanamori, *Phys. Rev. B* **63**, 180407(R) (2001).
- ²² N. A. Hill and K. M. Rabe, *Phys. Rev. B* **59**, 8759 (1999).
- ²³ R. Seshadri, NA Hill, *Chem. Mater.* **13**, 2892 (2001)
- ²⁴ P. W. Anderson, *Phys. Rev.* **79**, 350 (1950).
- ²⁵ *The Vienna ab-initio simulation package*, G. Kresse and J. Hafner, *Phys. Rev. B* **47**, R558 (1993); G. Kresse, Thesis, Technische Universität Wien (1993); G. Kresse and J. Furthmüller, *Comput. Mat. Sci.* **6**, 15 (1996); G. Kresse and J. Furthmüller, *Phys. Rev. B* **54**, 11169 (1996); G. Kresse, and D. Joubert, *Phys. Rev. B* **59**, 1758 (1999); P.E. Blöchl, *Phys. Rev. B* **50**, 17953 (1994).
- ²⁶ J. P. Perdew, K. Burke, and M. Ernzerhof, *Phys. Rev. Lett.* **77**, 3865 (1996).
- ²⁷ M. Ležaić, PhD Thesis, RWTH Aachen (2005).
- ²⁸ www.flapw.de
- ²⁹ F. Freimuth, Y. Mokrousov, D. Wortmann, S. Heinze, and S. Blügel, *Phys. Rev. B* **78**, 035120 (2008).
- ³⁰ C. J. Howard, B. J. Kennedy, and P. M. Woodward, *Acta Cryst. B* **59**, 463 (2003).
- ³¹ A. M. Glazer, *Acta Cryst. B* **28**, 3384 (1972)
- ³² P. Baettig and N. A. Spaldin, *Appl. Phys. Lett.* **86**, 012505 (2004).
- ³³ J. B. Goodenough, *Phys. Rev.* **100**, 564 (1955).
- ³⁴ J. Kanamori, *J. Phys. Chem. Solids* **10** 87 (1959).
- ³⁵ E. O. Wollan, *Phys. Rev.* **117**, 387 (1960).
- ³⁶ A. D. Rata, A. Herklotz, K. Nenkov, L. Schultz, and K. Dörr, *Phys. Rev. Lett.* **100**, 076401 (2008).
- ³⁷ Note that the lowest energy $P2_1/n$ structure would not be readily identified as the ground state through a search for unstable phonons starting from the prototype cubic perovskite structure because it only becomes lowest in energy when the lattice parameters are allowed to be unequal. Indeed, when we perform full structural optimizations within the LDA+U method for the previously studied double perovskite, $\text{Bi}_2\text{FeCrO}_6$ ³², we find the $P2_1/n$ structure to be lower in energy than the previously reported $R3$ when we allow for lattice parameters of different length. Interestingly, in this case, the GGA+U method yields a ferroelectric ground state, consistent with some experimental reports¹⁰.